

Ring-opening of Epoxides Mediated by Frustrated Lewis Pairs

Tetiana Krachko,^[a] Emmanuel Nicolas,^[a,b] Andreas W. Ehlers,^[a,c] Martin Nieger,^[d] and J. Chris Slootweg^{*[a]}

Abstract: Treatment of the preorganized frustrated Lewis pairs (FLPs) $t\text{Bu}_2\text{PCH}_2\text{BPh}_2$ (**1**) and $o\text{-Ph}_2\text{P}(\text{C}_6\text{H}_4)\text{BCat}$ (Cat = catechol) (**4**) with 2-methyloxirane, 2-phenyloxirane and 2-(trifluoromethyl)oxirane resulted in epoxide ring-opening to yield the six- and seven-membered heterocycles **2a–c** and **5a–c**, respectively. These zwitterionic products were characterized spectroscopically, and compounds **2a**, **2b**, **5a** and **5c** were structurally characterized by single-crystal X-ray structure analyses. Based on computational and kinetic studies, the mechanism of these reactions was found to proceed via activation of the epoxide by the Lewis acidic borane moiety followed by nucleophilic attack of the phosphine of a second FLP molecule. The resulting chain-like intermediates afford the final cyclic products by ring-closure and concurrent release of the second equivalent of FLP that behaves as catalyst in this reaction.

Introduction

Frustrated Lewis pairs (FLPs) are well-known metal-free compounds that can activate small molecule and this feature defines their intensive use in stoichiometric and catalytic main-group chemistry.¹ Accordingly, the combination of a Lewis acid and a Lewis base, which are sterically prevented from forming a classical Lewis acid-base adduct, allows the activation of a variety of small molecules,² including dihydrogen,^{2,3} olefins,⁴ alkynes,⁵ CO_2 ,⁶ SO_2 ,⁷ NO ,⁸ CO ,⁹ N_2O ,¹⁰ isocyanates, azides,¹¹ as well as singlet dioxygen.¹² Moreover, FLPs are also able to ring-open cyclic substrates. Stephan and co-workers showed that phosphine/borane¹³ or amine/borane¹⁴ combinations induce ring-opening of THF, while Tamm's group demonstrated that N-heterocyclic carbenes (NHCs) as Lewis bases can cleave THF in the presence of the highly electron-deficient tris(pentafluorophenyl)borane ($\text{B}(\text{C}_6\text{F}_5)_3$) affording in all cases zwitterionic species of type **A** (Figure 1).¹⁵ Analogous reactions of 1,4-dioxane or 1,4-thioxane with $\text{B}(\text{C}_6\text{F}_5)_3$ and an appropriate Lewis base result in C–O bond cleavage and the formation of ring-opened products of type **B** or **C**, respectively.^{14b} FLPs derived from P- or N-based Lewis bases and $\text{B}(\text{C}_6\text{F}_5)_3$ also induce ring-opening of δ -valerolactone to give zwitterionic

species **D**, while the analogous reactions with *rac*-lactide result in ring contraction to give salts of type **E**.¹⁶ Phosphine/borane FLPs also promote C–C bond scission of the three-membered cyclopropanes yielding the phosphonium borates **F** (Figure 1).¹⁷ Commonly, these ring-opening reactions occur via nucleophilic attack by a base on a Lewis acid-activated cyclic molecule. Furthermore, a cationic aluminium phosphine complex was shown to ring-open propylene oxide.¹⁸ Zhang, Darensbourg and co-workers extended this concept to catalytic ring-opening reactions, thereby developing the copolymerization of carbonyl sulfide and epoxides catalyzed by metal-free Lewis pairs.¹⁹ To further advance this field, a better mechanistic understanding of these ring-opening processes is desirable, which will aid in the development of more active and selective metal-free catalysts.

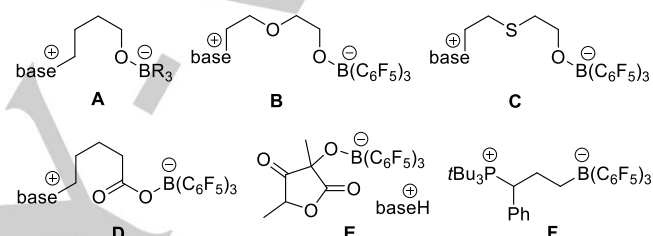


Figure 1. Examples of zwitterionic products resulting from the ring-opening reactions of FLPs with THF (**A**; base = phosphine, amine, NHC; $\text{BR}_3 = \text{B}(\text{C}_6\text{F}_5)_3$, $\text{B}(p\text{-C}_6\text{F}_4\text{H})_3$), dioxane (**B**; base = phosphine, amine), thioxane (**C**), δ -valerolactone (**D**), *rac*-lactide (**E**) and phenylcyclopropane (**F**).

Hence, we envisioned to examine the reactions of metal-free FLPs with epoxides, and study these reactions mechanistically by employing intramolecular FLPs. For this study, we chose the preorganized, non-fluorinated phosphinoborane $t\text{Bu}_2\text{PCH}_2\text{BPh}_2$ (**1**) developed in our group that exhibits typical FLP reactivity towards H_2 , CO_2 , isocyanates,²⁰ terminal alkynes, nitriles, and nitrilium salts.^{21, 22} In addition, the *ortho*-phenylene bridged phosphinoborane $o\text{-Ph}_2\text{P}(\text{C}_6\text{H}_4)\text{BCat}$ (Cat = catechol)²³ (**4**) bearing rather mild donor and acceptor sites was probed to study the influence of the FLP backbone and substituents on the reactivity. Herein, we describe the stoichiometric reactions of these two FLPs with mono-substituted epoxides and postulate the reaction mechanism based on DFT calculations and kinetic studies.

Results and Discussion

First, the reactivity of $t\text{Bu}_2\text{PCH}_2\text{BPh}_2$ (**1**) towards epoxides was investigated. Addition of 2-methyloxirane (propylene oxide; 4 equiv), 2-phenyloxirane (styrene oxide; 2 equiv) or 2-(trifluoromethyl)oxirane (4 equiv) to a toluene solution of **1** at 0 °C and stirring for 16–24 hours at room temperature afforded **2a–c** in 65%, 72% and 80% yield, respectively, after recrystallization (Scheme 1). The corresponding ¹¹B NMR spectra indicate the formation of tetracoordinate borate units displaying sharp singlets at –1.5 (**2a**), –1.4 (**2b**) and –1.2 ppm

[a] T. Krachko, Dr. E. Nicolas, Dr. A. W. Ehlers, Assoc. Prof. Dr. J. C. Slootweg

Van 't Hoff Institute for Molecular Sciences
University of Amsterdam, Science Park 904, PO Box 94157,
1090 GD Amsterdam (The Netherlands)
E-mail: j.c.slootweg@uva.nl

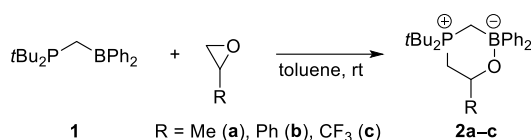
[b] Dr. E. Nicolas
current address: NIMBE, CEA, CNRS, Université Paris-Saclay,
CEA Saclay, 91191 Gif sur Yvette Cedex (France)

[c] Dr. A. W. Ehlers
Department of Chemistry, Science Faculty
University of Johannesburg
PO Box 254, Auckland Park, Johannesburg (South Africa)

[d] Dr. M. Nieger
Department of Chemistry University of Helsinki
A. I. Virtasen aukio 1, PO Box 55, Helsinki (Finland)

Supporting information for this article is given via a link at the end of the document.

(**2c**). The $^{31}\text{P}\{^1\text{H}\}$ NMR signals at 46.0 (**2a**), 46.3 (**2b**) and 46.5 ppm (**2c**) are consistent with the formation of tetracoordinate phosphonium centers. The ^{19}F NMR resonance of **2c** is shifted upfield from -75.4 to -79.9 ppm, which is indicative for 2-(trifluoromethyl)oxirane ring-opening.²⁴ The ^1H and $^1\text{H}\{^{31}\text{P}\}$ NMR spectra unambiguously confirms the methylene group of the 2-substituted oxiranes to be neighboring the P atom in the product ($^2J_{\text{H,P}} = 15.3$ (**2a**), 10.1 (**2b**), 11.5 (**2c**) Hz). In addition, the phenyl and *tert*-butyl groups as well as the protons of the methylene groups are all diastereotopic due to the presence of a stereogenic center in the molecule, and therefore provide distinct sets of signals in the ^1H NMR spectra.



Scheme 1. Reaction of FLP **1** with 2-methyloxirane (a), 2-phenyloxirane (b) and 2-(trifluoromethyl)oxirane (c).

The identification of **2a** and **2b** as cyclic zwitterionic phosphonium borates, resulting from a formal P/B FLP addition across the epoxide $\text{CH}_2\text{-O}$ bond, was also confirmed crystallographically (Figure 2).²⁵ The molecular structures show six-membered heterocycles in a distorted boat (**2a**) or chair conformation (**2b**) with typical B1–O1 and P1–C22 bond lengths of 1.4909(14) (**2a**), 1.4838(15) (**2b**) and 1.8179(11) (**2a**), 1.8228(12) Å (**2b**), respectively. Both crystallize in the $\text{P2}_1/n$ centrosymmetric space group, representing a racemic mixture of two enantiomers.

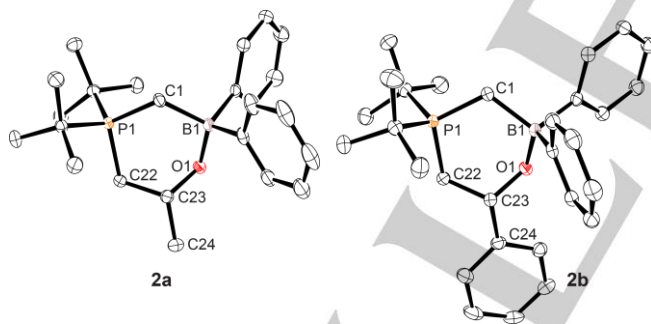
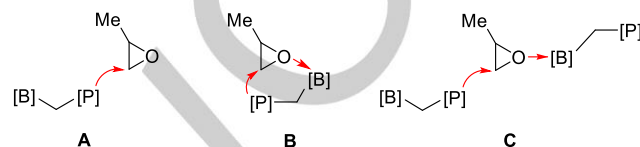


Figure 2. Molecular structures of **2a** and **2b** (one enantiomer is shown; ellipsoids are set at 50% probability, hydrogen atoms are omitted for clarity). Selected bond lengths [Å] and angles [°] for **2a**: P1–C22 1.8179(11), C22–C23 1.5400(15), C23–O1 1.4068(13), C23–C24 1.5220(15), O1–B1 1.4909(14), B1–C1 1.7023(16), C1–P1 1.7934(11); P1–C1–B1 115.77(7), P1–C22–C23 110.36(7), C22–C23–O1 107.78(9), C23–O1–B1 115.06(8). **2b**: P1–C22 1.8228(12), C22–C23 1.5479(15), C23–O1 1.4040(14), C23–C24 1.5223(16), O1–B1 1.4838(15), B1–C1 1.6924(17), C1–P1 1.7872(12); P1–C1–B1 115.77(8), P1–C22–C23 113.34(8), C22–C23–O1 110.02(9), C23–O1–B1 117.07(9).

To elucidate the mechanism of the epoxide ring-opening reaction mediated by FLP **1**, we performed $\omega\text{B97X-D/6-31G(d,p)}$ calculations in the gas phase.²⁸ We verified our computational method by performing single point calculations at

the $\omega\text{B97X-D/6-31G(d,p)}/\omega\text{B97X-D/6-31G(d,p)}$ level as well as included solvation effects (toluene), which in both cases gave similar relative Gibbs free energies (see Supporting Information). First, we focused on the ring-opening of 2-methyloxirane for which three possible pathways can be envisioned (Scheme 2).²⁹ Namely, the direct nucleophilic attack of a phosphorus nucleophile (**A**), activation of the epoxide by the Lewis acid followed by intramolecular nucleophilic attack by the Lewis base (**B**), and Lewis acid activation of the epoxide followed by intermolecular nucleophilic attack by the Lewis base of a second FLP moiety (**C**).



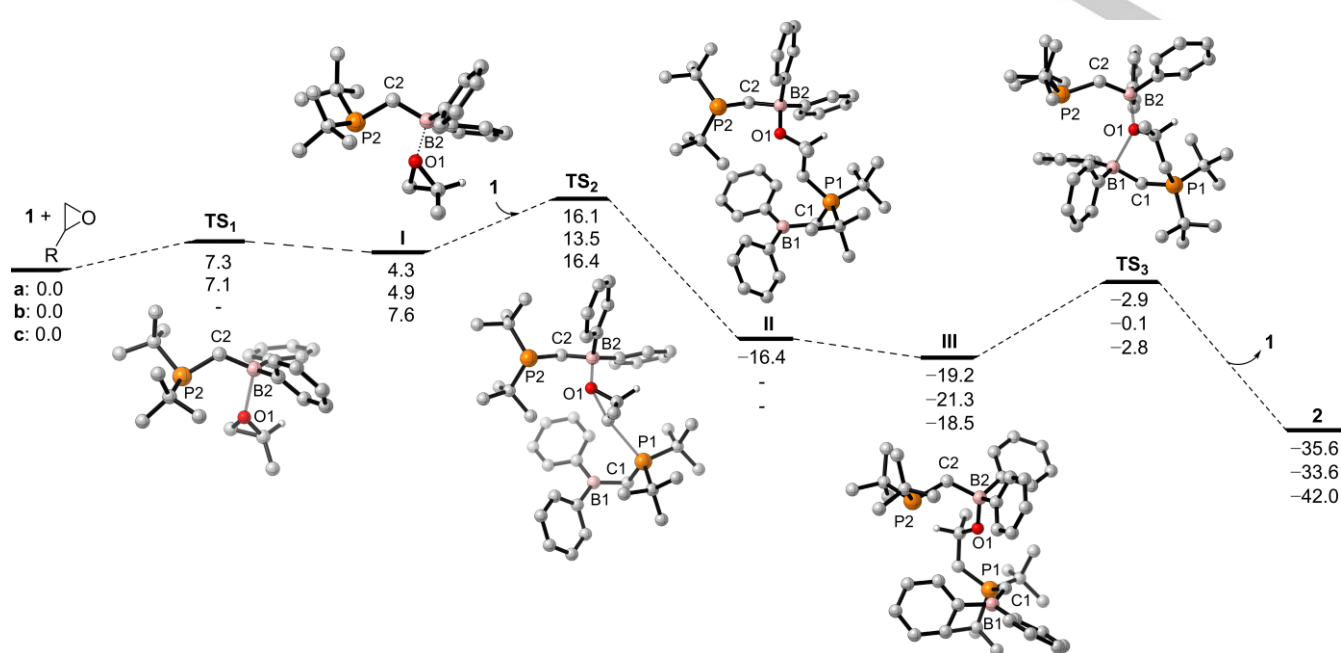
Scheme 2. Three epoxide ring-opening pathways. [P] = $\text{P}t\text{Bu}_2$; [B] = BPh_2 .

While strong anionic phosphorus nucleophiles, such as diphenylphosphide, have proven their effectiveness in epoxide ring-opening reactions,³⁰ reports on the employment of phosphines for this process are absent. Therefore, we were not surprised when our computations revealed that the direct C–O bond scission by P-nucleophilic attack of $t\text{Bu}_2\text{PCH}_2\text{BPh}_2$ (**1**) is a high-energy process that requires an activation barrier of $\Delta G^\ddagger = 44.4$ kcal·mol⁻¹, making route **A** unlikely (see the Supporting information for further details).

Next, we evaluated routes **B** and **C** which involve the initial activation of the epoxide by the Lewis acidic boron moiety of **1**. We found that activation can be achieved by the formation of Lewis adduct **1a** ($\Delta G = 4.3$ kcal·mol⁻¹, $\Delta G^\ddagger = 7.3$ kcal·mol⁻¹; Scheme 3) that displays a slightly elongated C22–O1 bond of 1.44 Å (vs. 1.42 Å in 2-methyloxirane). The next step is a nucleophilic attack of the phosphine on the least hindered epoxide C atom followed by ring opening. The activation energy required for C–O bond scission by intramolecular nucleophilic attack (Path **B**, see the Supporting information) is high (**TS_{1-2a}**: $\Delta G^\ddagger = 33.1$ kcal·mol⁻¹), this is the result of hampered orbital overlap of the $\sigma^*(\text{C-O})$ and the lone pair on the P atom. In contrast, the intermolecular nucleophilic attack of an additional FLP molecule has a substantially lower barrier (**TS_{2a}**: $\Delta G^\ddagger = 16.1$ kcal·mol⁻¹; Scheme 3), and is, therefore, the preferred reaction pathway for this process. The nucleophilic attack of the second FLP moiety occurs from the backside of the epoxide, maximizing overlap with the σ^* orbital of the C–O bond, resulting in the formation of the chain-like intermediate **11a** ($\Delta G = -16.4$ kcal·mol⁻¹; Scheme 3), which rearranges by rotation along the B2–O1 and B1–C1 bond to the more stable conformer **111a** ($\Delta G = -19.2$ kcal·mol⁻¹). Finally, the formation of product **2a** ($\Delta G = -35.6$ kcal·mol⁻¹) occurs by ring-closure with simultaneous release of the second FLP moiety. The activation barrier for this final step (**TS_{3a}**: $\Delta G^\ddagger = 16.3$ kcal·mol⁻¹) is comparable to the initial ring-opening of the epoxide ($\Delta G^\ddagger = 16.1$ kcal·mol⁻¹) and the magnitude of these barriers is fully consistent with the mild reaction conditions observed experimentally (room temperature, 16 hours). Note that the nucleophilic attack by the phosphine on

the more hindered, tertiary carbon of the epoxide is disfavored ($\Delta G^\ddagger = 26.7 \text{ kcal}\cdot\text{mol}^{-1}$, see the Supporting information), which is in line with the isolation of only one regioisomer. Overall, FLP

$t\text{Bu}_2\text{PCH}_2\text{BPh}_2$ (**1**) acts in this reaction both as stoichiometric reagent and catalyst at the same time.



Scheme 3. Relative $\omega\text{B97X-D/6-31G(d,p)}$ Gibbs free energies (in kcal mol⁻¹) for the conversion of **1** into **2a-c** (only the methyl-substituted species **a** are shown; hydrogen atoms are omitted for clarity).

To support the notion that epoxide ring-opening is induced by the action of a Lewis acidic borane and a Lewis basic phosphine from two separated FLP molecules, we performed the same reaction but now with a bimolecular FLP that mimics $t\text{Bu}_2\text{PCH}_2\text{BPh}_2$ (**1**). Thus, treatment of a toluene solution of triphenylborane with 2-methyloxirane, followed by the addition of di-*tert*-butylmethylphosphine afforded after 20 minutes at room temperature the zwitterionic phosphonium borate **3a** in 82% isolated yield ($\delta^{31}\text{P} = 44.8 \text{ ppm}$, $\delta^{11}\text{B} = 1.0 \text{ ppm}$; Figure 3). The molecular structure of **3a** is unambiguously established by single-crystal X-ray diffraction analysis (Figure 3, bottom)²⁵ and shows that the ring-opened 2-methyloxirane gives rise to slightly elongated B1–O1 (1.519(2) Å) and P1–C22 bonds (1.8192(17) Å) compared to the ones of **2a** (1.4909(14) and 1.8179(11) Å, respectively). The formation of **3a** supports our proposed mechanism for the formation of **2a** (Scheme 3), and it is interesting to note that the structure of **3a** is similar to the ones of the proposed intermediates **IIa** and **IIIa**.

Next, we investigated the mechanism of the reaction of 2-phenyloxirane with FLP **1**. Calculations at $\omega\text{B97X-D/6-31G(d,p)}$ revealed that 2-phenyloxirane also forms Lewis adduct **IIb** ($\Delta G = 4.9 \text{ kcal}\cdot\text{mol}^{-1}$, $\Delta G^\ddagger = 7.1 \text{ kcal}\cdot\text{mol}^{-1}$; Scheme 3), which after epoxide ring-opening directly affords intermediate **IIIb** ($\Delta G = -21.3 \text{ kcal}\cdot\text{mol}^{-1}$, $\Delta G^\ddagger = 13.5 \text{ kcal}\cdot\text{mol}^{-1}$). Subsequent cyclization with concomitant release of the second FLP moiety affords the final product **2b** ($\Delta G = -33.6 \text{ kcal}\cdot\text{mol}^{-1}$, $\Delta G^\ddagger = 21.2 \text{ kcal}\cdot\text{mol}^{-1}$). Compared to 2-methyloxirane, the activation barrier for the ring-opening step (TS_{2b}) of 2-phenyloxirane is slightly lower ($\Delta\Delta G = -2.6 \text{ kcal}\cdot\text{mol}^{-1}$), likely due to the higher basicity of 2-

phenyloxirane, while TS_{3b} for product formation is higher ($\Delta\Delta G = +4.9 \text{ kcal}\cdot\text{mol}^{-1}$) and becomes the rate-determining step.

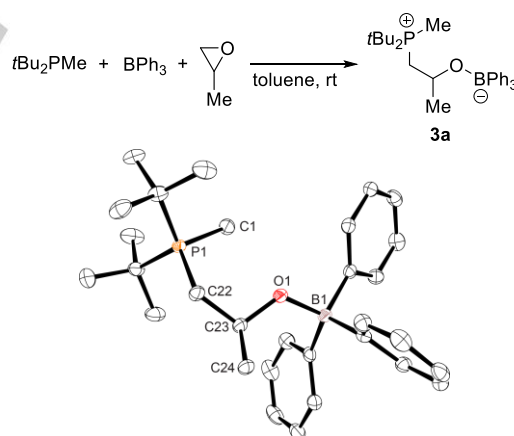


Figure 3. Reaction of $\text{BPh}_3/t\text{Bu}_2\text{PMe}$ with 2-methyloxirane (top) and molecular structure of **3a** (bottom; ellipsoids are set at 50% probability, hydrogen atoms are omitted for clarity). Selected bond lengths [Å] and angle [°] for **3a**: P1–C22 1.8192(17), C22–C23 1.538(2), C23–O1 1.403(2), C23–C24 1.532(2), O1–B1 1.519(2), C1–P1 1.7956(19); P1–C22–C23 118.56(12), C22–C23–O1 107.67(15), C23–O1–B1 119.77(14).

To gain further insight into the formation of **2b**, we performed kinetic studies³¹ and monitored the FLP concentration for a stoichiometric mixture of **1** and 2-phenyloxirane in toluene at 30 °C using $^{31}\text{P}\{^1\text{H}\}$ NMR spectroscopy. We found that the FLP

concentration decay is following first-order kinetics (Figure 4) with a rate constant of $6.01 \cdot 10^{-3} \text{ s}^{-1}$ that, by using the Eyring equation, provides an activation barrier of $\Delta G^\ddagger = 20.8 \text{ kcal}\cdot\text{mol}^{-1}$. These findings are consistent with our DFT calculations that also predicted a unimolecular process to be the rate-determining step (**TS**_{3b}: $\Delta G^\ddagger = 21.2 \text{ kcal}\cdot\text{mol}^{-1}$).

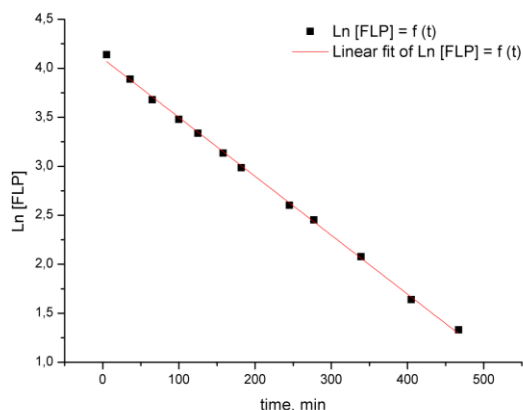
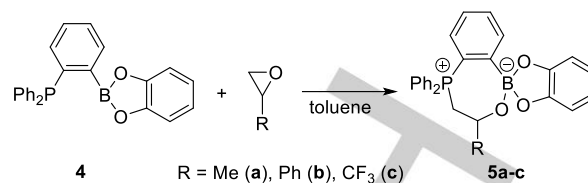


Figure 4. Plot of natural logarithm of FLP (**1**) concentration versus time determined by $^{31}\text{P}\{^1\text{H}\}$ NMR spectroscopy for the reaction of **1** (1 equiv) with 2-phenyloxirane (1 equiv). Slope (k) = $6.01 \cdot 10^{-3} \text{ s}^{-1}$, $R = 0.99874$.

Similar to **2a**, the reaction pathway for the formation of **2c** from 2-(trifluoromethyl)oxirane and **1** features activation barriers of comparable Gibbs free energy, **TS**_{2c} ($\Delta G^\ddagger = 16.4 \text{ kcal}\cdot\text{mol}^{-1}$) and **TS**_{3c} ($\Delta G^\ddagger = 15.7 \text{ kcal}\cdot\text{mol}^{-1}$). Consistently, kinetic data on this system show that the FLP concentration decrease corresponds neither to a first nor second order reaction type, indicating a more complicated reaction rate.³¹

To assess the influence of the FLP backbone and substituents on the reaction, *o*-phenylene-bridged FLP *o*-Ph₂P(C₆H₄)BCat (**4**) was treated with 2-methyloxirane, 2-phenyloxirane and 2-(trifluoromethyl)oxirane. As expected, the reduced Lewis acidity and basicity of **4** compared to **1** led to longer reaction times. The reactions with 2-methyl- and 2-phenyloxirane were completed after 72 and 24 hours at room temperature, respectively, whereas 2-(trifluoromethyl)oxirane required 72 hours at 70 °C for full conversion. The corresponding ring-opened products **5a** and **5c** were isolated in 90% and 85% yield (Scheme 4), respectively, while **5b** was obtained in 20% yield, likely due to the formation of oligomeric chains as side product.³² The ^{11}B NMR signals at 10.0 (**5a**, **5c**) and 10.5 ppm (**5b**) and the ^{31}P NMR resonances at 25.8 (**5a**), 32.0 (**5b**) and 25.6 (**5c**) ppm are in agreement with the formation of phosphonium borates akin to **2**. X-ray diffraction analysis of suitable crystals of **5a** and **5c** confirmed the formation of zwitterionic seven-membered heterocycles (Figure 5),²⁵ which display typical B1–O1(3) (1.457(3) Å and 1.476(2) Å, respectively) and P1–C25 bonds (1.809(2) Å and 1.8154(15) Å, resp) and show that the PCCB plane of the FLP moiety (P1–C2–C1–B1 –3.2(3)° (**5a**) and 1.3(2)° (**5c**)) is orthogonal to the C25–C26–O1(3) plane of the ring-opened epoxide.



Scheme 4. Reaction of FLP **4** with 2-methyloxirane (**a**), 2-phenyloxirane (**b**) and 2-(trifluoromethyl)oxirane (**c**).

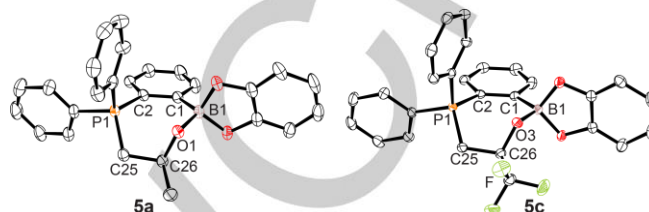


Figure 5. Molecular structures of **5a** and **5c** (one enantiomer is shown; ellipsoids are set at 50% probability, hydrogen atoms and CHCl₃ solvent molecule are omitted for clarity). Selected bond lengths [Å] and angles [°] for **5a**: P1–C25 1.809(2), C25–C26 1.529(3), C26–O1 1.422(3), O1–B1 1.457(3), B1–C1 1.628(3), C1–C2 1.405(3), C2–P1 1.804(2); C2–P1–C25 112.53(10), O1–B1–C1 113.37(18), C25–C26–O1 108.00(17); B1–C1–C2–P1 –3.2(3). **5c**: P1–C25 1.8154(15), C25–C26 1.528(2), C26–O3 1.3911(18), O3–B1 1.476(2), B1–C1 1.626(2), C1–C2 1.406(2), C2–P1 1.8057(15); C2–P1–C25 115.67(7), O3–B1–C1 112.58(12), C25–C26–O3 109.81(11); B1–C1–C2–P1 1.3(2).

ω B97X-D/6-31G(d,p) calculations for the formation of **5a** revealed some interesting differences compared to the formation of **2a** (see the Supporting information). First, the activation barrier for ring-opening is increased (**TS**₂: $\Delta G^\ddagger = 20.4 \text{ kcal}\cdot\text{mol}^{-1}$ (**5a**) vs $16.1 \text{ kcal}\cdot\text{mol}^{-1}$ (**2a**)), due to the reduced P-nucleophilicity of **4**. Second, product formation by cyclization of intermediate **III** and elimination of the second FLP moiety is in this case a much more facile process (**TS**₃: $\Delta G^\ddagger = 5.1 \text{ kcal}\cdot\text{mol}^{-1}$ (**5a**) vs $16.3 \text{ kcal}\cdot\text{mol}^{-1}$ (**2a**)), likely due to the reduced electrophilicity of **4** that promotes its release from the reaction site. As a result, epoxide ring-opening by the second equivalent of FLP becomes the rate-limiting step (see the Supporting Information). This is supported by kinetic data which shows that the FLP concentration decay follows second-order kinetics (Figure 6) with a rate constant of $8.41 \cdot 10^{-6} \text{ s}^{-1}$ ($\Delta G^\ddagger = 24.3 \text{ kcal}\cdot\text{mol}^{-1}$), which is consistent with a rate-limiting bimolecular process.

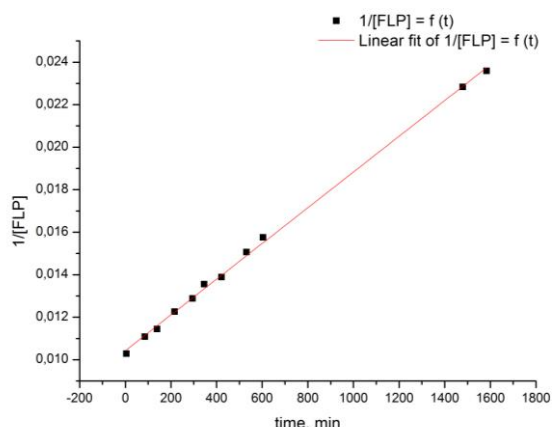


Figure 6. Plot of inverse FLP (**4**) concentration ($1/[\text{FLP}]$) versus time determined by ^{31}P NMR spectroscopy for the reaction of **4** (1 equiv) with 2-methyloxirane (1 equiv). Slope (k) = $8.41 \cdot 10^{-6} \text{ s}^{-1}$, $R = 0.99869$.

After observing these facile FLP-mediated epoxide ring-opening reactions, we were keen to learn whether this mode of action is also operational for the higher homologues of the substrate. We found that the P/B-based FLP $t\text{Bu}_2\text{PCH}_2\text{BPh}_2$ (**1**) is also reactive towards the sulfur analogues of epoxides (episulfides) that are applied in industrial copolymerization processes,³³ but that the reaction follows a different course.³⁴ Namely, treatment of a toluene solution of **1** with propylene sulfide (2.8 equiv) afforded after 2 hours at room temperature and work-up zwitterionic product **6** ($\delta^{31}\text{P} = 79.4$ ppm, $\delta^{11}\text{B} = 8.2$ ppm; Figure 7) in 94% isolated yield. The molecular structure of **6** obtained by an X-ray crystal structure determination (Figure 7, right)²⁵ unequivocally established the formation of a planar four-membered heterocycle (S1–P1–C1–B1 $0.92(11)^\circ$) with the sulfur atom in the bridging position between the P and B atoms, which points out that the FLP-mediated ring-opening of heterocyclopropanes is tunable and can be converted into a heteroatom transfer reaction.

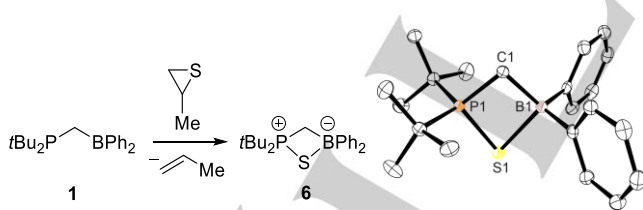


Figure 7. Reaction of **1** with propylene sulfide (left) and molecular structure of **6** (right; ellipsoids are set at 50% probability, hydrogen atoms are omitted for clarity). Selected bond lengths [Å] and angle [°] for **6**: P1–S1 2.0280(5), S1–B1 2.1117(19), B1–C1 1.670(2), C1–P1 1.7875(16); P1–S1–B1 75.48(5), S1–B1–C1 95.45(10), B1–C1–P1 94.23(10), C1–P1–S1 94.83(6); S1–P1–C1–B1 $0.92(11)$.

Conclusions

In this study, the reactivity of intramolecular P/B-based FLPs towards mono-substituted epoxides has been explored, which resulted in the formation of zwitterionic six- and seven-

membered heterocycles that are obtained regioselectively upon epoxide ring-opening. The mechanism of this reaction has been assessed computationally and is supported by kinetic studies, showing that the FLP behaves simultaneously as a stoichiometric reagent and catalyst in this process. We found that the rate-determining step of the reaction is strongly dependent on the Lewis acidity and basicity of the FLP as well as the basicity of the epoxide, which shows these are important design principles, while the nature of the heterocyclopropanes can also determine the reaction outcome. These findings will stimulate the advancement of (co)polymerization of epoxides mediated by metal-free (frustrated) Lewis pairs knowing that these systems can be readily tuned by varying the strength of the available Lewis acidic and basic sites.

Experimental Section

General methods and materials: All syntheses were carried out under an atmosphere of dry nitrogen employing standard Schlenk-line and glovebox techniques. Solvents were purified, dried and degassed according to standard procedures. ^1H and $^{13}\text{C}\{^1\text{H}\}$ NMR spectra were recorded on a Bruker Avance 500 or Bruker Avance 400 and internally referenced to the residual solvent resonances (CDCl_3 : ^1H δ 7.26 ppm, $^{13}\text{C}\{^1\text{H}\}$ δ 77.16 ppm; CD_2Cl_2 : ^1H δ 5.32 ppm, $^{13}\text{C}\{^1\text{H}\}$ δ 53.84 ppm). $^{31}\text{P}\{^1\text{H}\}$, $^{11}\text{B}\{^1\text{H}\}$ spectra were recorded on a Bruker Avance 400 and externally referenced (85% H_3PO_4 and $\text{BF}_3 \cdot \text{OEt}_2$, respectively). ^{19}F NMR spectra were recorded on a Bruker Avance 250 and externally referenced (CFCl_3). The ^1H and ^{13}C resonance signals were attributed by means of 2D HSQC and HMBC experiments. Melting points were measured on samples in sealed capillaries on a Stuart Scientific SMP3 melting point apparatus and are uncorrected. High resolution mass spectra (HRMS) were recorded on a Bruker Daltonics micrOTOF spectrometer using electrospray ionization (ESI).

$t\text{Bu}_2\text{PCH}_2\text{BPh}_2$ (**1**)²⁰ and $o\text{-Ph}_2\text{P}(\text{C}_6\text{H}_4)\text{BCat}$ (**4**)²³ were prepared according to literature procedures. All epoxides as racemic mixtures were purchased from commercial resources and stored over activated 3Å molecular sieves.

Synthesis of 2a: A solution of 2-methyloxirane (0.345 mL, 4.93 mmol, 4.0 equiv) in toluene (5 mL) was added dropwise to a solution of **1** (0.400 g, 1.23 mmol, 1.0 equiv) in toluene (5 mL) at 0°C . Then the reaction mixture was allowed to warm to room temperature. After subsequent stirring overnight at room temperature, the excess of 2-methyloxirane and half of toluene were removed under reduced pressure. Cooling to -20°C resulted in the deposition of white crystals which were collected by filtration, washed with cold toluene (2 x 5 mL) and *n*-pentane (2 x 5 mL) to give **2a** as a white solid in 65% yield (0.306 g, 0.800 mmol). Crystals suitable for single X-ray diffraction were grown by vapor diffusion of pentane into a concentrated solution of **2a** in DCM. **M.p.:** 199–203 $^\circ\text{C}$. **^1H NMR** (500.2 MHz, CDCl_3 , 293 K): δ 7.55 (d, $^3J_{\text{H,H}} = 7.5$ Hz, 2H; *o*- C_6H_5), 7.46 (d, $^3J_{\text{H,H}} = 7.5$ Hz, 2H; *o*- C_6H_5), 7.18 (t, $^3J_{\text{H,H}} = 7.4$ Hz, 2H; *m*- C_6H_5), 7.09 (t, $^3J_{\text{H,H}} = 7.5$ Hz, 2H; *m*- C_6H_5), 7.02 (t, $^3J_{\text{H,H}} = 7.2$ Hz, 1H; *p*- C_6H_5), 6.92 (t, $^3J_{\text{H,H}} = 7.2$ Hz, 1H; *p*- C_6H_5), 3.78 (m, 1H; $\text{CH}(\text{CH}_3)$), 1.73 (m, 2H; CH_2CH), 1.47 (dd, $^3J_{\text{H,H}} = 5.9$ Hz, $^4J_{\text{H,P}} = 2.9$ Hz, 3H; $\text{CH}(\text{CH}_3)$), 1.31 (dd, $^2J_{\text{H,H}} = ^2J_{\text{H,P}} = 15.1$ Hz, 1H; $\text{PCHH}'\text{B}$), 1.25 (d, $^3J_{\text{H,P}} = 16.5$ Hz, 9H; $\text{C}(\text{CH}_3)_3$), 1.21 (d, $^3J_{\text{H,P}} = 16.5$ Hz, 9H; $\text{C}(\text{CH}_3)_3$), 1.13 (dd, $^2J_{\text{H,H}} = ^2J_{\text{H,P}} = 15.3$ Hz, 1H; $\text{PCHH}'\text{B}$). **$^{11}\text{B}\{^1\text{H}\}$ NMR** (128.4 MHz, CDCl_3 , 293 K): δ -1.5

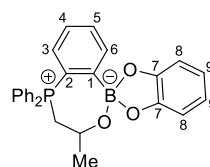
(s). $^{13}\text{C}\{^1\text{H}\}$ NMR (125.8 MHz CDCl_3 , 293 K): δ 160.2 (br. s; *ipso*- C_6H_5), 159.5 (br. s; *ipso*- C_6H_5), 131.5 (s; *o*- C_6H_5), 130.9 (s; *o*- C_6H_5), 126.9 (s; *m*- C_6H_5), 126.6 (s; *m*- C_6H_5), 123.8 (s; *p*- C_6H_5), 123.5 (s; *p*- C_6H_5), 63.8 (d, $^2J_{\text{C,P}} = 4.9$ Hz; $\text{CH}(\text{CH}_3)$), 33.8 (d, $^1J_{\text{C,P}} = 37.1$ Hz; $\text{C}(\text{CH}_3)_3$), 33.2 (d, $^1J_{\text{C,P}} = 39.0$ Hz; $\text{C}(\text{CH}_3)_3$), 27.0 (d, $^3J_{\text{C,P}} = 12.1$ Hz; $\text{CH}(\text{CH}_3)$), 26.9 (s; $\text{C}(\text{CH}_3)_3$), 26.8 (s; $\text{C}(\text{CH}_3)_3$), 21.7 (d, $^1J_{\text{C,P}} = 48.4$ Hz; CH_2CH), -0.4 (d, $^1J_{\text{C,P}} = 47.0$ Hz; PCH_2B). $^{31}\text{P}\{^1\text{H}\}$ NMR (162.0 MHz, CDCl_3 , 293 K): δ 46.0 (s). **HR ESI-MS**: calcd for $\text{C}_{24}\text{H}_{37}\text{BOP}$ (M+H) 383.2674, found 383.2689. *m/z* (%): 383.3 (8) $[\text{M}+\text{H}]^+$, 305.2 (18) $[\text{M}-\text{C}_6\text{H}_5]^+$, 219.2 (24) $[\text{M}-\text{BPh}_2]^+$, 175.2 (100) $[\text{P}(\text{tBu})_2(\text{CH}_3)_2]^+$.

Synthesis of 2b: A solution of 2-phenyloxirane (0.280 mL, 2.46 mmol, 2.0 equiv) in toluene (5 mL) was added dropwise to a solution of **1** (0.400 g, 1.23 mmol, 1.0 equiv) in toluene (5 mL) at 0 °C. Then the reaction mixture was allowed to warm to room temperature. After subsequent stirring overnight at room temperature, the reaction mixture was concentrated to half of its original volume. Cooling to -20 °C resulted in the deposition of colorless crystals which were collected by filtration, washed with cold toluene (2 x 5 mL) and *n*-pentane (2 x 5 mL) at -20 °C to give **2b** in 72% yield (0.393 g, 0.884 mmol). Crystallization from toluene at room temperature afforded X-ray quality crystals. **M.p.**: 198–199 °C. **^1H NMR** (500.2 MHz, CDCl_3 , 293 K): δ 7.66 (d, $^3J_{\text{H,H}} = 7.5$ Hz, 2H; *o*- C_6H_5), 7.65 (d, $^3J_{\text{H,H}} = 7.2$ Hz, 2H; *o*- C_6H_5), 7.48 (d, $^3J_{\text{H,H}} = 7.0$ Hz, 2H; *o*- $\text{CH}(\text{C}_6\text{H}_5)$), 7.42 (t, $^3J_{\text{H,H}} = 7.6$ Hz, 2H; *m*- $\text{CH}(\text{C}_6\text{H}_5)$), 7.31 (t, $^3J_{\text{H,H}} = 7.3$ Hz, 1H; *p*- $\text{CH}(\text{C}_6\text{H}_5)$), 7.14 (t, $^3J_{\text{H,H}} = 7.4$ Hz, 2H; *m*- C_6H_5), 7.10 (t, $^3J_{\text{H,H}} = 7.4$ Hz, 2H; *m*- C_6H_5), 6.96 (t, $^3J_{\text{H,H}} = 7.2$ Hz, 1H; *p*- C_6H_5), 6.97 (t, $^3J_{\text{H,H}} = 7.2$ Hz, 1H; *p*- C_6H_5), 4.78 (ddd, $^3J_{\text{H,H}} = 11.0$ Hz, $^3J_{\text{H,H}} = 2.5$ Hz, $^3J_{\text{H,P}} = 2.5$ Hz, 1H; $\text{CH}(\text{C}_6\text{H}_5)$), 1.97 (m, 2H; CH_2CH), 1.45 (dd, $^2J_{\text{H,H}} = ^2J_{\text{H,P}} = 15.0$ Hz, 1H; $\text{PCHH}'\text{B}$), 1.33 (d, $^3J_{\text{H,P}} = 13.7$ Hz, 9H; $\text{C}(\text{CH}_3)_3$), 1.26 (dd, $^2J_{\text{H,H}} = ^2J_{\text{H,P}} = 15.3$ Hz, 1H; $\text{PCHH}'\text{B}$), 1.19 (d, $^3J_{\text{H,P}} = 14.3$ Hz, 9H; $\text{C}(\text{CH}_3)_3$). **$^{11}\text{B}\{^1\text{H}\}$ NMR** (128.4 MHz, CDCl_3 , 293 K): δ -1.4 (s). **$^{13}\text{C}\{^1\text{H}\}$ NMR** (125.8 MHz, CDCl_3 , 293 K): δ 160.7 (s; *ipso*- $\text{B}(\text{C}_6\text{H}_5)$), 159.5 (s; *ipso*- $\text{B}(\text{C}_6\text{H}_5)$), 147.7 (d, $^3J_{\text{C,P}} = 10.5$ Hz; *ipso*- $\text{CH}(\text{C}_6\text{H}_5)$), 131.4 (s; *o*- $\text{CH}(\text{C}_6\text{H}_5)$), 130.9 (s; *o*- $\text{B}(\text{C}_6\text{H}_5)$), 128.5 (s; *m*- $\text{CH}(\text{C}_6\text{H}_5)$), 127.0 (s; *m*- $\text{B}(\text{C}_6\text{H}_5)$), 126.8 (s; *p*- $\text{CH}(\text{C}_6\text{H}_5)$), 125.6 (s; *o*- $\text{B}(\text{C}_6\text{H}_5)$), 123.8 (s; *p*- $\text{B}(\text{C}_6\text{H}_5)$), 123.5 (s; *p*- $\text{B}(\text{C}_6\text{H}_5)$), 69.5 (d, $^2J_{\text{C,P}} = 4.3$ Hz; $\text{CH}(\text{CH}_3)$), 34.1 (d, $^1J_{\text{C,P}} = 36.5$ Hz; $\text{C}(\text{CH}_3)_3$), 33.2 (d, $^1J_{\text{C,P}} = 38.8$ Hz; $\text{C}(\text{CH}_3)_3$), 26.9 (d, $^2J_{\text{C,P}} = 9.5$ Hz; $\text{C}(\text{CH}_3)_3$), 23.3 (d, $^1J_{\text{C,P}} = 45.3$ Hz; CH_2CH), 0.7 (br. s; PCH_2B). Carbon atoms directly attached to boron (*ipso*- $\text{B}(\text{C}_6\text{H}_5)$ and PCH_2B) are not observed in direct ^{13}C NMR spectra, but are seen in HMBC and HSQC experiments. **$^{31}\text{P}\{^1\text{H}\}$ NMR** (162.0 MHz, CDCl_3 , 293 K): δ 46.3 (s). **HR ESI-MS**: calcd for $\text{C}_{29}\text{H}_{39}\text{BOP}$ (M+H) 445.2831, found 445.2851. *m/z* (%): 445.3 (1) $[\text{M}+\text{H}]^+$, 367.2 (100) $[\text{M}-\text{C}_6\text{H}_5]^+$, 281.2 (92) $[\text{M}-\text{BPh}_2]^+$, 175.2 (10) $[\text{P}(\text{tBu})_2(\text{CH}_3)_2]^+$.

Synthesis of 2c: A solution of **1** (0.300 g, 0.925 mmol, 1.0 equiv) in pentane (5 mL) was added dropwise to a solution of 2-(trifluoromethyl)oxirane (0.320 mL, 3.70 mmol, 4.0 equiv) in pentane (5 mL) at 0 °C. After the addition was completed, the reaction was allowed to stir at room temperature for 24 hours. During that time the initially colorless solution became pink with a pale pink precipitate. The reaction solution was filtered over a glass frit and washed with cold pentane (3 x 5 mL). Afterwards, the residue was recrystallized from warm ethanol (10 mL) to give **2c** as beige crystals in 80% yield (0.322 g, 0.740 mmol). **M.p.**: >164 °C (decomp.). **^1H NMR** (400.0 MHz, CDCl_3 , 293 K): δ 7.56 (d, $^3J_{\text{H,H}} = 7.6$ Hz, 2H; *o*- C_6H_5), 7.46 (d, $^3J_{\text{H,H}} = 7.6$ Hz, 2H; *o*- C_6H_5), 7.19 (t, $^3J_{\text{H,H}} = 7.4$ Hz, 2H; *m*- C_6H_5), 7.10 (t, $^3J_{\text{H,H}} = 7.4$ Hz, 2H; *m*- C_6H_5), 7.03 (td, $^3J_{\text{H,H}} = 7.3$ Hz, $^4J_{\text{H,H}} = 1.2$ Hz, 1H; *p*- C_6H_5), 6.94 (td, $^3J_{\text{H,H}} = 7.3$ Hz, $^4J_{\text{H,H}}$

= 1.3 Hz, 1H; *p*- C_6H_5), 4.11 (m, 1H; $\text{CH}(\text{CF}_3)$), 2.07 (ddd, $^2J_{\text{H,H}} = 14.7$ Hz, $^3J_{\text{H,H}} = 11.6$ Hz, $^2J_{\text{H,P}} = 11.5$ Hz, 1H; $\text{CH}'\text{HCH}$), 1.84 (ddd, $^2J_{\text{H,H}} = 14.8$ Hz, $^3J_{\text{H,H}} = 2.2$ Hz, $^2J_{\text{H,P}} = 10.6$ Hz, 1H; $\text{CH}'\text{HCH}$), 1.45 (dd, $^2J_{\text{H,H}} = ^2J_{\text{H,P}} = 15.2$ Hz, 1H; $\text{PCHH}'\text{B}$), 1.29 (d, $^3J_{\text{H,P}} = 14.1$ Hz, 9H; $\text{C}(\text{CH}_3)_3$), 1.22 (d, $^3J_{\text{H,P}} = 14.7$ Hz, 9H; $\text{C}(\text{CH}_3)_3$), 1.19 (dd, $^2J_{\text{H,H}} = ^2J_{\text{H,P}} = 15.6$ Hz, 1H; $\text{PCHH}'\text{B}$). **$^{11}\text{B}\{^1\text{H}\}$ NMR** (128.4 MHz, CDCl_3 , 293 K): δ -1.2 (s). **$^{13}\text{C}\{^1\text{H}\}$ NMR** (101 MHz, CDCl_3 , 293 K): δ 158.9 (s; *ipso*- C_6H_5), 156.9 (s; *ipso*- C_6H_5), 131.7 (s; *o*- C_6H_5), 130.7 (s; *o*- C_6H_5), 127.3 (s; *m*- C_6H_5), 126.9 (s; *m*- C_6H_5), 125.7 (q, $^1J_{\text{C,F}} = 269.8$ Hz; CF_3), 124.4 (s; *p*- C_6H_5), 123.8 (s; *p*- C_6H_5), 68.0 (qd, $^2J_{\text{C,F}} = 31.2$, $^2J_{\text{C,P}} = 3.9$ Hz; CH), 34.3 (d, $^1J_{\text{C,P}} = 37.3$ Hz; $\text{C}(\text{CH}_3)_3$), 33.7 (d, $^1J_{\text{C,P}} = 39.4$ Hz; $\text{C}(\text{CH}_3)_3$), 26.8 (s; $\text{C}(\text{CH}_3)_3$), 26.7 (s; $\text{C}(\text{CH}_3)_3$), 13.8 (dq, $^1J_{\text{C,P}} = 52.8$ Hz, $^3J_{\text{C,F}} = 1.5$ Hz; CH_2CH), -0.4 (PCH_2B). **^{19}F NMR** (235.3 MHz, CDCl_3 , 296 K) δ -79.9 (d, $^3J_{\text{F,H}} = 6.0$ Hz). **$^{31}\text{P}\{^1\text{H}\}$ NMR** (162.0 MHz, CDCl_3 , 293 K): δ 46.5 (s). **HR ESI-MS**: calcd for $\text{C}_{18}\text{H}_{28}\text{BF}_3\text{OP}$ (M-C $_6\text{H}_5$) 359.1921, found 359.1903. *m/z* (%): 273.2 (100) $[\text{M}-\text{BPh}_2]^+$, 359.2 (5) $[\text{M}-\text{C}_6\text{H}_5]^+$.

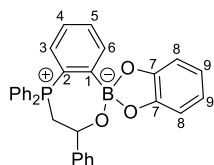
Synthesis of 3a: 2-Methyloxirane (0.12 mL, 1.65 mmol, 2.0 equiv) was added dropwise to a solution of triphenylborane (200 mg, 0.826 mmol, 1.0 equiv) in toluene (4 mL) at -60 °C, followed by the addition of a solution of di-*tert*-butylmethylphosphine (0.16 mL, 0.823 mmol, 1.0 equiv) in toluene (6 mL) at the same temperature. The resulting mixture was stirred for 10 min at -60 °C, after which it was allowed to warm to room temperature. After subsequent stirring for 20 min at room temperature, a white precipitation had formed. The suspension was cooled down to -60 °C, and then all white crystals were collected by filtration and washed with toluene (3 x 5 mL) and *n*-pentane (2 x 5 mL) to give **3a** in 82% yield (0.312 g, 0.678 mmol). To increase the purity even further, the residue can also be recrystallized from layering a saturated DCM solution of **3a** with *n*-pentane. Suitable crystals for single X-ray diffraction were grown by vapor diffusion of pentane into a concentrated solution of **3a** in DCM. **M.p.**: >173 °C (decomposition). **^1H NMR** (400.0 MHz, CD_2Cl_2 , 293 K): δ 7.49 (d, $^3J_{\text{H,H}} = 7.3$ Hz, 6H; *o*- C_6H_5), 7.08 (t, $^3J_{\text{H,H}} = 7.3$ Hz, 6H; *m*- C_6H_5), 6.95 (t, $^3J_{\text{H,H}} = 7.2$ Hz, 3H; *p*- C_6H_5), 3.69–3.54 (m, 1H; $\text{CH}(\text{CH}_3)$), 2.37 (ddd, $^2J_{\text{H,H}} = 15.3$ Hz, $^3J_{\text{H,H}} = ^2J_{\text{H,P}} = 9.7$ Hz, 1H; CHH'), 1.86 (dd, $^2J_{\text{H,H}} = 15.3$ Hz, $^2J_{\text{H,P}} = 9.7$ Hz, 1H; CHH'), 1.68 (d, $^2J_{\text{H,P}} = 12.7$ Hz, 3H; PCH_3), 1.42 (d, $^3J_{\text{H,P}} = 14.8$, 9H; $\text{C}(\text{CH}_3)_3$), 1.14 (dd, $^3J_{\text{H,H}} = 5.8$ Hz, $^4J_{\text{H,P}} = 1.8$ Hz, 3H; $\text{CH}(\text{CH}_3)$), 1.10 (d, $^3J_{\text{H,P}} = 14.5$ Hz, 9H; $\text{C}(\text{CH}_3)_3$). **$^{11}\text{B}\{^1\text{H}\}$ NMR** (128.4 MHz, CD_2Cl_2 , 293 K): δ 1.0 (s). **$^{13}\text{C}\{^1\text{H}\}$ NMR** (125.8 MHz, CD_2Cl_2 , 293 K): δ 161.0 (br. s; *ipso*- C_6H_5), 134.6 (s; *o*- C_6H_5), 126.3 (s; *m*- C_6H_5), 123.3 (s; *p*- C_6H_5), 65.4 (d, $^2J_{\text{C,P}} = 6.0$ Hz; $\text{CH}(\text{CH}_3)$), 33.6 (d, $^1J_{\text{C,P}} = 39.7$ Hz; $\text{C}(\text{CH}_3)_3$), 33.3 (d, $^1J_{\text{C,P}} = 39.7$ Hz; $\text{C}(\text{CH}_3)_3$), 27.1 (d, $^1J_{\text{C,P}} = 42.3$ Hz; CH_2), 27.1 (d, $^3J_{\text{C,P}} = 14.6$ Hz; $\text{CH}(\text{CH}_3)$), 26.7 (d, $^2J_{\text{C,P}} = 13.2$ Hz; $\text{C}(\text{CH}_3)_3$), -0.1 (d, $^1J_{\text{C,P}} = 46.9$ Hz; PCH_3). **$^{31}\text{P}\{^1\text{H}\}$ NMR** (162.0 MHz, CD_2Cl_2 , 293 K): δ 44.8 (s). **HR ESI-MS**: calcd for $\text{C}_{12}\text{H}_{28}\text{PO}$ (M-BPh $_3$ +H) 219.1878, found 219.1889. *m/z* (%): 243.1 (100) $[\text{BPh}_3+\text{H}]^+$, 219.2 (100) $[\text{M}-\text{BPh}_3+\text{H}]^+$, 175.2 (10) $[\text{P}(\text{tBu})_2(\text{CH}_3)_2]^+$.



Synthesis of 5a: A solution of 2-methyloxirane (0.220 mL, 3.16 mmol, 4.0 equiv) in toluene (3 mL) was added dropwise to a solution of **4** (0.300 g, 0.789 mmol, 1.0 equiv) in toluene (17 mL) at room temperature. After the addition was completed, the reaction was allowed to stir at room temperature for 72 hours, at which time the slurry was concentrated to half of its original volume and filtered over a glass frit. The collected solid was washed with

cold toluene (3 x 10 mL) and pentane (3 x 5 mL) to give **5a** as a colorless powder in 90% yield (0.311 g, 0.710 mmol). Crystallization from dichloromethane/*n*-pentane at room temperature afforded X-ray quality crystals. **M.p.:** 233 °C. **¹H NMR** (500.0 MHz, CDCl₃, 293 K): δ 7.99 (dd, ³J_{H,H} = 7.2 Hz, ⁴J_{H,P} = 4.4 Hz, 1H; *H^β*), 7.73 (td, ³J_{H,H} = 7.5 Hz, ⁴J_{H,H} = 1.1 Hz, 1H; *p*-C₆H₅), 7.71–7.64 (m, 1H; *p*-C₆H₅), 7.64–7.53 (m, 7H; *o*-C₆H₅, *m*-C₆H₅, *H^β*), 7.45 (dd, ³J_{H,H} = 7.7 Hz, ³J_{H,P} = 11.7 Hz, 2H; *o*-C₆H₅), 7.20 (td, ³J_{H,H} = 7.6 Hz, ⁴J_{H,P} = 3.8 Hz, 1H; *H^α*), 6.77 (dd, ³J_{H,H} = 7.9 Hz, ²J_{H,P} = 14.2 Hz, 1H; *H^β*), 6.66 (br. s, 2H; *H^β*), 6.61–6.54 (m; 2H, *H^β*), 4.58 (sep, ³J_{H,H} = 6.8 Hz, 1H; CH(CH₃)), 3.47 (dd, ³J_{H,H} = 7.9 Hz, ²J_{H,P} = 12.3 Hz, 2H; CH₂), 1.31 (dd, ³J_{H,H} = 6.2 Hz, ⁴J_{H,H} = 1.6 Hz, 3H; CH₃). **¹¹B{¹H} NMR** (128.4 MHz, CDCl₃, 293 K): δ 10.0 (s). **¹³C{¹H} NMR** (125.8 MHz CDCl₃, 293 K): δ 160.7 (br. s; C¹), 153.1 (s, C⁷), 136.5 (d, ³J_{C,P} = 16.3 Hz; C⁶), 133.9 (s; *p*-C₆H₅), 133.9 (d, ²J_{C,P} = 8.8 Hz; *o*-C₆H₅), 133.8 (s; C⁵), 133.5 (s; *p*-C₆H₅), 133.4 (d, ²J_{C,P} = 18.7 Hz; C³), 132.9 (d, ³J_{C,P} = 10.2 Hz; *m*-C₆H₅), 129.9 (d, ³J_{C,P} = 11.4 Hz; *m*-C₆H₅), 129.7 (d, ²J_{C,P} = 13.1 Hz; *o*-C₆H₅), 127.3 (d, ³J_{C,P} = 13.8 Hz; C⁴), 123.8 (d, ¹J_{C,P} = 70.2 Hz; *ipso*-C₆H₅), 123.1 (d, ¹J_{C,P} = 59.9 Hz; *ipso*-C₆H₅), 118.4 (s, C²), 117.7 (s; C⁹), 109.1 (s; C⁸), 61.4 (d, ²J_{C,P} = 6.8 Hz; CH(CH₃)), 39.6 (d, ¹J_{C,P} = 58.9 Hz; CH₂), 24.8 (d, ³J_{C,P} = 11.1 Hz; CH₃). **³¹P{¹H} NMR** (162.0 MHz, CDCl₃, 293 K): δ 25.8 (s). **HR ESI-MS:** calcd for C₂₇H₂₅BO₃P (M+H) 439.1634, found 439.1626. *m/z* (%): 439.2 (1) [M+H]⁺, 347.1 (100) [M-OC₆H₄+H]⁺.

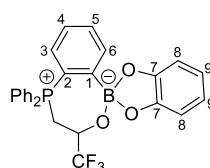
Synthesis of 5b: A solution of 2-phenyloxirane (0.180 mL, 1.58 mmol, 2.0 equiv) in toluene (3 mL) was added dropwise to a solution of **4** (0.300 g, 0.789 mmol, 1.0 equiv) in toluene (17 mL) at room temperature. After the addition was completed, the reaction was allowed to stir for 24 hours at room temperature, at which time the slurry was filtered over a glass frit.



The collected solid was washed with cold toluene (3 x 10 mL) and pentane (3 x 5 mL) and afterwards the product was extracted from this solid into DCM (2 x 10 mL). Removal of the solvent *in vacuo* gave **5b** as a white powder in 20% yield (0.079 g, 0.158 mmol). **M.p.:** 240 °C. **¹H NMR** (400 MHz, CD₂Cl₂, 293 K): δ 7.88 (dd, ³J_{H,H} = 7.4 Hz, ⁴J_{H,P} = 4.4 Hz, 1H; *H^β*), 7.79–7.70 (m, 1H; *H^β*), 7.67–7.56 (m, 6H; *o*-P(C₆H₅), *m*-P(C₆H₅), *p*-P(C₆H₅)₂), 7.38 (td, ³J_{H,H} = 7.9 Hz, ⁴J_{H,P} = 3.5 Hz, 2H; *m*-P(C₆H₅)), 7.34–7.16 (m, 6H; C⁴, *o*-CH(C₆H₅), *m*-CH(C₆H₅), *p*-CH(C₆H₅)), 7.05 (ddd, ³J_{H,H} = 8.0 Hz, ⁴J_{H,H} = 1.1 Hz, ³J_{H,P} = 12.4 Hz, 2H; *o*-P(C₆H₅)), 6.80 (dd, ³J_{H,H} = 8.0 Hz, ³J_{H,P} = 13.6 Hz, 1H; *H^β*), 6.68–6.49 (m, 4H; *H^β*, *H^β*), 5.08 (td, ³J_{H,H} = 6.0 Hz, ³J_{H,P} = 12.8 Hz, 1H; CH(C₆H₅)), 4.62 (ddd, ²J_{H,H} = 11.5 Hz, ³J_{H,H} = 6.6 Hz, ²J_{H,P} = 15.5 Hz, 1H; CHH'P), 4.31 (ddd, ²J_{H,H} = 11.5 Hz, ³J_{H,H} = 5.3 Hz, ²J_{H,P} = 17.0 Hz, 1H; CHH'P). **¹¹B{¹H} NMR** (128.4 MHz, CD₂Cl₂, 293 K): δ 10.5 (s). **¹³C{¹H} NMR** (101.0 MHz CD₂Cl₂, 293 K): δ 153.8 (s; C⁷), 136.6 (d, ³J_{C,P} = 16.2 Hz; C⁶), 135.5 (d, ²J_{C,P} = 9.1 Hz; *o*-P(C₆H₅)), 134.7 (d, ³J_{C,P} = 8.3 Hz; *m*-P(C₆H₅)), 134.4 (d, ²J_{C,P} = 14.7 Hz; C³), 134.0 (d, ⁴J_{C,P} = 2.9 Hz; C⁵), 133.8 (s; *p*-P(C₆H₅)), 133.7 (s; *p*-P(C₆H₅)), 133.7 (d, ³J_{C,P} = 6.9 Hz; *ipso*-CH(C₆H₅)), 130.6 (d, ⁴J_{C,P} = 5.6 Hz; *o*-CH(C₆H₅)), 130.0 (d, ²J_{C,P} = 11.6 Hz; *o*-P(C₆H₅)), 129.3 (d, ⁵J_{C,P} = 3.0 Hz; *m*-CH(C₆H₅)), 129.1 (d, ⁶J_{C,P} = 3.7 Hz; *p*-CH(C₆H₅)), 128.9 (d, ³J_{C,P} = 12.4 Hz; *m*-P(C₆H₅)), 127.8 (d, ³J_{C,P} = 13.2 Hz; C⁴), 123.1 (d, ¹J_{C,P} = 82.1 Hz; *ipso*-C₆H₅), 120.5 (d, ¹J_{C,P} = 76.7 Hz; *ipso*-C₆H₅), 119.6 (d, ¹J_{C,P} = 73.6 Hz; C²), 118.0 (s; C⁹), 108.9 (s; C⁸), 108.8 (s; C⁶), 62.2 (d, ¹J_{C,P} = 6.8 Hz; CH₂), 53.1 (s; CH(C₆H₅)). **³¹P{¹H} NMR** (162.0 MHz, CD₂Cl₂, 293 K): δ 32.0 (s). **HR ESI-MS:** calcd for

C₃₂H₂₇BO₃P (M+H) 501.1791, found 501.1787. *m/z* (%): 501.2 (2) [M+H]⁺, 409.2 (100) [M-OC₆H₄+H]⁺.

Synthesis of 5c: A solution of 2-(trifluoromethyl)oxirane (0.280 mL, 3.23



mmol, 4.0 equiv) in toluene (3 mL) was added dropwise to a solution of **4** (0.300 g, 0.789 mmol, 1.0 equiv) in toluene (17 mL) at room temperature. After the addition was completed, the reaction was left to stir in a closed vessel at 70 °C for 72 hours, at which

time the slurry was concentrated to half of its original volume and filtered over a glass frit. The collected solid was washed with cold toluene (3 x 10 mL) and pentane (3 x 5 mL) to give **5c** as a white powder in 85% yield (0.330 g, 0.671 mmol). Crystallization from chloroform at room temperature afforded X-ray quality crystals. **M.p.:** 245 °C. **¹H NMR** (400.0 MHz, CDCl₃, 293 K): δ 8.01 (dd, ³J_{H,H} = 6.8 Hz, ⁴J_{H,P} = 4.7 Hz, 1H; *H^β*), 7.78 (td, ³J_{H,H} = 7.4 Hz, ⁴J_{H,H} = 1.3 Hz, 1H; *p*-C₆H₅), 7.75–7.69 (m, 1H; *p*-C₆H₅), 7.68–7.55 (m, 7H; *o*-C₆H₅, *m*-C₆H₅, *H^β*), 7.45 (dd, ³J_{H,H} = 7.4 Hz, ³J_{H,P} = 11.9, 2H; *o*-C₆H₅), 7.26 (tdd, ³J_{H,H} = 7.7 Hz, ⁴J_{H,H} = 1.3 Hz, ⁴J_{H,P} = 3.8 Hz, 1H; *H^α*), 6.81 (dd, ³J_{H,H} = 7.8 Hz, ³J_{H,P} = 14.4 Hz, 1H; *H^β*), 6.72 (d, ³J_{H,H} = 7.1 Hz, 1H; *H^β*), 6.64–6.54 (m, 3H; *H^β*, *H^β*), 4.95 (m, 1H; CH(CF₃)), 3.76 (ddd, ²J_{H,H} = ²J_{H,P} = 15.2 Hz, ³J_{H,H} = 9.0 Hz; CHH'), 3.49 (ddd, ²J_{H,H} = 15.4 Hz, ²J_{H,P} = 11.2 Hz, ³J_{H,H} = 5.9 Hz, 1H; CHH'). **¹¹B{¹H} NMR** (128.4 MHz, CDCl₃, 293 K): δ 10.0 (s). **¹³C{¹H} NMR** (101.0 MHz CDCl₃, 293 K): δ 159.2 (br. S; C¹), 152.8 (s; C⁷), 152.6 (s; C⁷), 137.1 (d, ³J_{C,P} = 16.4 Hz; C⁶), 134.6 (d, ⁴J_{C,P} = 3.5 Hz; *p*-C₆H₅), 134.5 (d, ⁴J_{C,P} = 2.8 Hz; *p*-C₆H₅), 134.0 (s; C⁵), 134.0 (d, ²J_{C,P} = 11.3 Hz; *o*-C₆H₅), 133.6 (d, ²J_{C,P} = 16.1 Hz; C³), 132.7 (d, ³J_{C,P} = 10.6 Hz; *m*-C₆H₅), 130.2 (d, ³J_{C,P} = 11.6 Hz; *m*-C₆H₅), 129.9 (d, ²J_{C,P} = 13.5 Hz; *o*-C₆H₅), 127.8 (d, ³J_{C,P} = 14.0 Hz; C⁴), 125.0 (qd, ¹J_{C,F} = 282.1 Hz, ⁴J_{C,P} = 12.8 Hz; CF₃), 122.2 (d, ¹J_{C,P} = 88.3 Hz; *ipso*-C₆H₅), 122.1 (d, ¹J_{C,P} = 89.3 Hz; *ipso*-C₆H₅), 118.1 (s; C⁹), 118.0 (s; C⁹), 116.9 (d, ¹J_{C,P} = 87.6 Hz; C²), 109.7 (s; C⁶), 108.9 (s; C⁶), 64.3 (qd, ²J_{C,F} = 33.9 Hz, ¹J_{C,P} = 6.1 Hz; CH(CF₃)), 32.7 (d, ¹J_{C,P} = 64.3 Hz; CH₂); C¹ is not observed in direct ¹³C NMR spectra, but is seen in HMBC at 159.2 ppm. **³¹P{¹H} NMR** (162.0 MHz, CDCl₃, 293 K): δ 25.6 (s). **¹⁹F NMR** (235.3 MHz, CDCl₃, 293 K): δ -78.9 (dd, ³J_{F,H} = 6.8 Hz, ⁴J_{F,P} = 1.0 Hz). **HR ESI-MS:** calcd for C₂₇H₂₂BF₃O₃P (M+H) 493.1351, found 493.1359. *m/z* (%): 801.2 (100) [2M-2(OC₆H₄+H)]⁺, 493.1 (3) [M+H]⁺, 401.1 (34) [M-OC₆H₄+H]⁺.

Synthesis of 6: A solution of propylene sulfide (0.200 mL, 2.55 mmol, 2.8 equiv) in pentane (5 mL) was added dropwise to a solution of **1** (0.300 g, 0.925 mmol, 1.0 equiv) in pentane (5 mL) at -78 °C. Then the reaction mixture was allowed to warm to room temperature. After subsequent stirring for 2 hours at room temperature, the reaction solution was filtered over a glass frit and washed with pentane (3 x 5 mL) to give **6** as a white powder in 94% yield (0.310 g, 0.870 mmol). Suitable crystals for single X-ray diffraction were grown by vapor diffusion of pentane into a concentrated solution of **6** in DCM. **M.p.:** >75 °C (decomposition). **¹H NMR** (400.1 MHz, CD₂Cl₂, 298 K): δ 7.50 (d, ³J_{H,H} = 7.8 Hz, 4H; *o*-C₆H₅), 7.20 (t, ³J_{H,H} = 7.3 Hz, 4H; *m*-C₆H₅), 7.06 (tt, ³J_{H,H} = 7.3 Hz, ⁴J_{H,H} = 1.3 Hz, 2H; *p*-C₆H₅), 2.08 (d, ²J_{H,P} = 12.8 Hz, 2H; CH₂), 1.26 (d, ³J_{H,P} = 16.0 Hz, 18H; C(CH₃)₃). **¹¹B{¹H} NMR** (96.3 MHz, CDCl₃, 295 K): δ 8.2 (s). **¹³C{¹H} NMR** (100.6 MHz, CD₂Cl₂, 298 K): δ 154.2 (br. s; *ipso*-C₆H₅), 131.1 (s; *o*-C₆H₅), 127.3 (s; *m*-C₆H₅), 125.0 (s; *p*-C₆H₅), 37.4 (d, ¹J_{C,P} = 26.6 Hz; C(CH₃)₃), 26.5 (d, ²J_{C,P} = 2.9 Hz; C(CH₃)₃), 9.4 (br. s.; CH₂). **³¹P{¹H} NMR** (121.5 MHz, CDCl₃, 295 K): δ 79.4 (s).

X-ray crystal structure determination

The single-crystal X-ray diffraction studies were carried out on a Bruker D8 Venture diffractometer with Photon100 detector at 123(2) K using Cu-K α radiation (**2b**, **3a**, **5a**, **5c**, **6**, $\lambda = 1.54178 \text{ \AA}$) or on a Bruker-Nonius KappaCCD diffractometer at 123(2) K using Mo-K α radiation (**2a**, $\lambda = 0.71073 \text{ \AA}$). Direct Methods (SHELXS-97 for **2a**, **2b**, **5c**, **6**)³⁵ or dual space methods (SHELXT for **3a**, **5a**)³⁶ were used for structure solution and refinement was carried out using SHELXL-2014 (full-matrix least-squares on F^2).³⁷ Hydrogen atoms were localized by difference electron density determination and refined using a riding model. Semi-empirical absorption corrections were applied. For **3a** and **5c** an extinction correction were applied. The absolute configuration was determined by refinement of Parsons' x-parameter for **3a**.³⁸ **6** was refined as a 2-component inversion twin (see cif-files for details). In **5a** the refinement with the listed atoms show residual electron density due to 4 heavily disordered solvent molecules CH₂Cl₂ in 4 voids around the 2-fold axis which could not be refined with split atoms. Therefore the option "SQUEEZE" of the program package PLATON³⁹ was used to create a hkl file taking into account the residual electron density in the void areas. Therefore the atoms list and unit card do not agree (see cif-file for details).

2a: colorless crystals, C₂₄H₃₆BOP, $M_r = 382.31$, crystal size 0.60 × 0.40 × 0.30 mm, monoclinic, space group $P2_1/n$ (No. 14), $a = 9.2155(9) \text{ \AA}$, $b = 13.6724(13) \text{ \AA}$, $c = 17.8492(14) \text{ \AA}$, $\beta = 97.724(9)^\circ$, $V = 2228.6(4) \text{ \AA}^3$, $Z = 4$, $\rho = 1.139 \text{ Mg/m}^{-3}$, $\mu(\text{Cu-K}\alpha) = 0.134 \text{ mm}^{-1}$, $F(000) = 832$, $2\theta_{\text{max}} = 55.0^\circ$, 37166 reflections, of which 5107 were independent ($R_{\text{int}} = 0.025$), 244 parameters, $R_1 = 0.034$ (for 4520 $I > 2\sigma(I)$), $wR_2 = 0.090$ (all data), $S = 1.04$, largest diff. peak / hole = $0.381 / -0.229 \text{ e \AA}^{-3}$.

2b: colorless crystals, C₂₉H₃₈BOP, $M_r = 444.37$, crystal size 0.20 × 0.20 × 0.16 mm, monoclinic, space group $P2_1/n$ (No. 14), $a = 10.9530(4) \text{ \AA}$, $b = 17.0757(6) \text{ \AA}$, $c = 13.6498(5) \text{ \AA}$, $\beta = 96.909(1)^\circ$, $V = 2534.39(16) \text{ \AA}^3$, $Z = 4$, $\rho = 1.165 \text{ Mg/m}^{-3}$, $\mu(\text{Cu-K}\alpha) = 1.082 \text{ mm}^{-1}$, $F(000) = 960$, $2\theta_{\text{max}} = 144.0^\circ$, 29159 reflections, of which 4963 were independent ($R_{\text{int}} = 0.024$), 289 parameters, $R_1 = 0.034$ (for 4792 $I > 2\sigma(I)$), $wR_2 = 0.091$ (all data), $S = 1.03$, largest diff. peak / hole = $0.314 / -0.307 \text{ e \AA}^{-3}$.

3a: colorless crystals, C₃₀H₄₂BOP, $M_r = 460.41$, crystal size 0.30 × 0.20 × 0.20 mm, monoclinic, space group $P2_1$ (No. 4), $a = 8.1258(4) \text{ \AA}$, $b = 17.2320(8) \text{ \AA}$, $c = 9.6507(5) \text{ \AA}$, $\beta = 97.231(1)^\circ$, $V = 1340.58(11) \text{ \AA}^3$, $Z = 2$, $\rho = 1.141 \text{ Mg/m}^{-3}$, $\mu(\text{Cu-K}\alpha) = 1.037 \text{ mm}^{-1}$, $F(000) = 500$, $2\theta_{\text{max}} = 144.4^\circ$, 19505 reflections, of which 5256 were independent ($R_{\text{int}} = 0.022$), 299 parameters, 1 restraint, $R_1 = 0.028$ (for 5230 $I > 2\sigma(I)$), $wR_2 = 0.075$ (all data), $S = 1.04$, largest diff. peak / hole = $0.245 / -0.186 \text{ e \AA}^{-3}$, $x = 0.010(7)$.

5a: colorless crystals, C₂₇H₂₄BO₃P · 0.5(CH₂Cl₂), $M_r = 480.70$, crystal size 0.20 × 0.06 × 0.03 mm, monoclinic, space group $C2/c$ (No. 15), $a = 33.9262(8) \text{ \AA}$, $b = 8.5134(2) \text{ \AA}$, $c = 21.8006(6) \text{ \AA}$, $\beta = 128.529(3)^\circ$, $V = 4925.8(3) \text{ \AA}^3$, $Z = 8$, $\rho = 1.296 \text{ Mg/m}^{-3}$, $\mu(\text{Cu-K}\alpha) = 2.203 \text{ mm}^{-1}$, $F(000) = 2008$, $2\theta_{\text{max}} = 144.2^\circ$, 26102 reflections, of which 4850 were independent ($R_{\text{int}} = 0.044$), 290 parameters, $R_1 = 0.053$ (for 4134 $I > 2\sigma(I)$), $wR_2 = 0.133$ (all data), $S = 1.07$, largest diff. peak / hole = $0.500 / -0.345 \text{ e \AA}^{-3}$.

5c: colorless crystals, C₂₇H₂₁BF₃O₃P · CHCl₃, $M_r = 611.58$, crystal size 0.40 × 0.22 × 0.16 mm, triclinic, space group $P-1$ (No. 2), $a = 9.6170(7) \text{ \AA}$, $b = 10.6466(7) \text{ \AA}$, $c = 14.2544(10) \text{ \AA}$, $\alpha = 105.414(2)^\circ$, $\beta = 96.649(2)^\circ$, $\gamma = 102.231(2)^\circ$, $V = 1361.92(16) \text{ \AA}^3$, $Z = 2$, $\rho = 1.502 \text{ Mg/m}^{-3}$, $\mu(\text{Cu-K}\alpha) = 4.080 \text{ mm}^{-1}$, $F(000) = 624$, $2\theta_{\text{max}} = 144.6^\circ$, 40985 reflections, of which 5320 were independent ($R_{\text{int}} = 0.028$), 353 parameters, $R_1 = 0.031$ (for 5091 $I > 2\sigma(I)$), $wR_2 = 0.078$ (all data), $S = 1.03$, largest diff. peak / hole = $0.637 / -0.619 \text{ e \AA}^{-3}$.

6: colorless crystals, C₂₁H₃₀BPS, $M_r = 356.29$, crystal size 0.32 × 0.08 × 0.04 mm, orthorhombic, space group $P2_12_12_1$ (No. 19), $a = 9.7345(5) \text{ \AA}$, $b = 11.9393(6) \text{ \AA}$, $c = 17.1612(8) \text{ \AA}$, $V = 1994.53(17) \text{ \AA}^3$, $Z = 4$, $\rho = 1.187 \text{ Mg/m}^{-3}$, $\mu(\text{Cu-K}\alpha) = 2.166 \text{ mm}^{-1}$, $F(000) = 768$, $2\theta_{\text{max}} = 144.2^\circ$, 24944 reflections, of which 3918 were independent ($R_{\text{int}} = 0.026$), 218 parameters, $R_1 = 0.023$ (for 3892 $I > 2\sigma(I)$), $wR_2 = 0.062$ (all data), $S = 1.07$, largest diff. peak / hole = $0.211 / -0.284 \text{ e \AA}^{-3}$, inversion twin, $x = 0.489(16)$.

CCDC 1827770 (**2a**), 1827771 (**2b**), 1827772 (**3a**), 1827773 (**5a**), 1827774 (**5c**), and 1827775 (**6**) contain the supplementary crystallographic data for this paper. These data can be obtained free of charge from The Cambridge Crystallographic Data Centre via www.ccdc.cam.ac.uk/data_request/cif.

Acknowledgements

This work was supported financially by the European Union (Marie Curie ITN SusPhos, Grant Agreement No. 317404) and the Council for Chemical Sciences of The Netherlands Organization for Scientific Research (NWO/CW) by a VIDJ grant (J.C.S.). We thank Kinga Kaniewska for her contribution to the synthesis of FLP **4**.

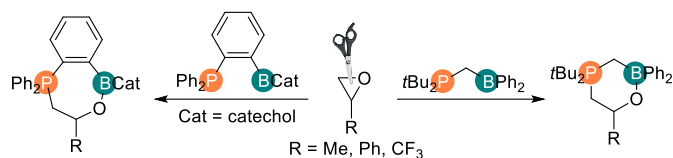
Keywords: Frustrated Lewis pairs • epoxides • ring-opening reactions • DFT calculations • kinetic studies

- [1] a) D. W. Stephan, *Acc. Chem. Res.* **2015**, *48*, 306–316. b) D. W. Stephan, *Science* **2016**, *354*, 1248; c) D. J. Scott, M. J. Fuchter, A. E. Ashley, *Chem. Soc. Rev.* **2017**, *46*, 5689–5700.
- [2] For reviews, see: a) D. W. Stephan, G. Erker, *Angew. Chem. Int. Ed.* **2015**, *54*, 6400–6441; b) G. Kehr, G. Erker, *Chem. Rec.* **2017**, *17*, 803–815; c) D. W. Stephan, G. Erker, *Chem. Sci.* **2014**, *5*, 2625–2641.
- [3] G. C. Welch, R. R. San Juan, J. D. Masuda, D. W. Stephan, *Science* **2006**, *314*, 1124–1126.
- [4] For selected examples, see: a) J. S. J. McCahill, G. C. Welch, D. W. Stephan, *Angew. Chem. Int. Ed.* **2007**, *46*, 4968–4971; b) A. Stirling, A. Hamza, T. A. Rokob, I. Pápai, *Chem. Commun.* **2008**, 3148–3150; c) C. M. Mömning, S. Frömel, G. Kehr, R. Fröhlich, S. Grimme, G. Erker, *J. Am. Chem. Soc.* **2009**, *131*, 12280–12289.
- [5] a) M. A. Dureen, D. W. Stephan, *J. Am. Chem. Soc.* **2009**, *131*, 8396–8397; b) E. R. M. Habraken, L. C. Mens, M. Nieger, M. Lutz, A. W. Ehlers, J. C. Slootweg, *Dalton Trans.* **2017**, *46*, 12284–12292; c) V. Fasano, L. D. Curless, J. E. Radcliffe, M. J. Ingleson, *Angew. Chem. Int. Ed.* **2017**, *56*, 9202–9206.
- [6] a) C. M. Mömning, E. Otten, G. Kehr, R. Fröhlich, S. Grimme, D. W. Stephan, G. Erker, *Angew. Chem. Int. Ed.* **2009**, *48*, 6643–6646; b) X. Zhao, D. W. Stephan, *Chem. Commun.* **2011**, *47*, 1833–1835.
- [7] M. Sajid, A. Klose, B. Birkmann, L. Liang, B. Schirmer, T. Wiegand, H. Eckert, A. J. Lough, R. Fröhlich, C. G. Daniliuc, S. Grimme, D. W. Stephan, G. Kehr, G. Erker, *Chem. Sci.* **2013**, *4*, 213–219.
- [8] a) A. J. P. Cardenas, B. J. Culotta, T. H. Warren, S. Grimme, A. Stute, R. Fröhlich, G. Kehr, G. Erker, *Angew. Chem. Int. Ed.* **2011**, *50*, 7567–7571; b) M. Sajid, A. Stute, A. J. P. Cardenas, B. J. Culotta, J. A. M. Hepperle, T. H. Warren, B. Schirmer, S. Grimme, A. Studer, C. G. Daniliuc, R. Fröhlich, J. L. Petersen, G. Kehr, G. Erker, *J. Am. Chem. Soc.* **2012**, *134*, 10156–10168; c) J. C. M. Pereira, M. Sajid, G. Kehr, A. M. Wright, B. Schirmer, Z.-W. Qu, S. Grimme, G. Erker, P. C. Ford, *J. Am. Chem. Soc.* **2014**, *136*, 513–519.

- [9] a) M. A. Dureen, D. W. Stephan, *J. Am. Chem. Soc.* **2010**, *132*, 13559–13568; b) M. Sajid, L.-M. Elmer, C. Rosorius, C. G. Daniliuc, S. Grimme, G. Kehr, G. Erker, *Angew. Chem. Int. Ed.* **2013**, *52*, 2243–2246.
- [10] a) E. Otten, R. C. Neu, D. W. Stephan, *J. Am. Chem. Soc.* **2009**, *131*, 9918–9919; b) R. C. Neu, E. Otten, A. Lough, D. W. Stephan, *Chem. Sci.* **2011**, *2*, 170–176; c) Z. Mo, E. L. Kolychev, A. Rit, J. Campos, H. Niu, S. Aldridge, *J. Am. Chem. Soc.* **2015**, *137*, 12227–12230.
- [11] a) C. M. Mömning, G. Kehr, B. Wibbeling, R. Fröhlich, G. Erker, *Dalton Trans.* **2010**, *39*, 7556; b) J. Zhou, L. L. Cao, L. (Leo) Liu, D. W. Stephan, *Dalton Trans.* **2017**, *46*, 9334–9338.
- [12] S. Porcel, G. Bouhadir, N. Saffon, L. Maron, D. Bourissou, *Angew. Chem. Int. Ed.* **2010**, *49*, 6186–6189.
- [13] a) G. C. Welch, J. D. Masuda, D. W. Stephan, *Inorg. Chem.* **2006**, *45*, 478–480; b) G. C. Welch, R. Prieto, M. A. Dureen, A. J. Lough, O. A. Labeodan, T. Höllricher-Rössmann, D. W. Stephan, *Dalton Trans.* **2009**, 1559–1570; c) X. Zhao, A. J. Lough, D. W. Stephan, *Chem. Eur. J.* **2011**, *17*, 6731–6743; d) M. J. Sgro, J. Dömer, D. W. Stephan, *Chem. Commun.* **2012**, *48*, 7253–7255.
- [14] a) S. J. Geier, D. W. Stephan, *J. Am. Chem. Soc.* **2009**, *131*, 3476–3477; b) B. Birkmann, T. Voss, S. J. Geier, M. Ullrich, G. Kehr, G. Erker, D. W. Stephan, *Organometallics* **2010**, *29*, 5310–5319.
- [15] a) D. Holschumacher, T. Bannenberg, C. G. Hrib, P. G. Jones, M. Tamm, *Angew. Chem. Int. Ed.* **2008**, *47*, 7428–7432; b) S. Kronig, E. Theuergarten, D. Holschumacher, T. Bannenberg, C. G. Daniliuc, P. G. Jones, M. Tamm, *Inorg. Chem.* **2011**, *50*, 7344–7359.
- [16] C. Kreitner, S. J. Geier, L. J. E. Stanlake, C. B. Caputo, D. W. Stephan, *Dalton Trans.* **2011**, *40*, 6771–6777.
- [17] J. G. M. Morton, M. A. Dureen, D. W. Stephan, *Chem. Commun.* **2010**, *46*, 8947–8949.
- [18] T. E. Stennett, J. Pahl, H. S. Zijlstra, F. W. Seidel, S. Harder, *Organometallics* **2016**, *35*, 207–217.
- [19] J.-L. Yang, H.-L. Wu, Y. Li, X.-H. Zhang, D. J. Darensbourg, *Angew. Chem. Int. Ed.* **2017**, *56*, 5774–5779.
- [20] F. Bertini, V. Lyaskovskyy, B. J. J. Timmer, F. J. J. de Kanter, M. Lütz, A. W. Ehlers, J. C. Slootweg, K. Lammertsma, *J. Am. Chem. Soc.* **2012**, *134*, 201–204.
- [21] E. R. M. Habraken, L. C. Mens, M. Nieger, M. Lutz, A. W. Ehlers, J. C. Slootweg, *Dalton Trans.* **2017**, *46*, 12284–12292.
- [22] For the reaction with CuCl, see: D. H. A. Boom, A. W. Ehlers, M. Nieger, J. C. Slootweg, *Z. Naturforsch., B: J. Chem. Sci.* **2017**, *72*, 781–784.
- [23] M. A. Courtemanche, M. A. Légaré, L. Maron, F. G. Fontaine, *J. Am. Chem. Soc.* **2013**, *135*, 9326–9329.
- [24] J. Rayó, L. Muñoz, G. Rosell, M. Bosch, Á. Guerrero, *Synthesis* **2010**, 3117–3120.
- [25] CCDC 1827770 (**2a**), 1827771 (**2b**), 1827772 (**3a**), 1827773 (**5a**), 1827774 (**5c**), and 1827775 (**6**) contain the supplementary crystallographic data for this paper. These data can be obtained free of charge from The Cambridge Crystallographic Data Centre via www.ccdc.cam.ac.uk/data_request/cif. For the experimental details of the X-ray crystal structure determinations, see the Supporting Information.
- [26] J.-D. Chai, M. Head-Gordon, *Phys. Chem. Chem. Phys.* **2008**, *10*, 6615–6620.
- [27] a) P. C. Hariharan, J. A. Pople, *Theor. Chim. Acta* **1973**, *28*, 213–222; b) M. M. Francl, W. J. Pietro, W. J. Hehre, J. S. Binkley, M. S. Gordon, D. J. DeFrees, J. A. Pople, *J. Chem. Phys.* **1982**, *77*, 3654–3665; c) W. J. Hehre, R. Ditchfield, J. A. Pople, *J. Chem. Phys.* **1972**, *56*, 2257–2261.
- [28] DFT calculations were carried out with Gaussian09 (Revision D.01); see the Supporting Information for further details.
- [29] For selected reviews and books on reactions of epoxides, see: a) R. E. Parker, N. S. Isaacs, *Chem. Rev.* **1959**, *59*, 737–799; b) B. H. Rotstein, S. Zaretsky, V. Rai, A. K. Yudin, *Chem. Rev.* **2014**, *114*, 8323–8359; c) T. W. Wilson, S. E. Denmark in *Lewis Base Catalysis in Organic Synthesis* (eds.: E. Vedejs and S. E. Denmark), Wiley-VCH Verlag GmbH & Co. KGaA, Weinheim, Germany, **2016**, pp. 1113–1152.
- [30] a) A. C. Connell, G. H. Whitham, *J. Chem. Soc. Perkin Trans. 1* **1983**, 989–994; b) H. Brunner, A. Sicheneder, *Angew. Chem. Int. Ed. Engl.* **1988**, *27*, 718–719; c) H. Fernández-Pérez, M. A. Pericàs, A. Vidal-Ferran, *Adv. Synth. Catal.* **2008**, *350*, 1984–1990; d) H. Fernández-Pérez, P. Etayo, J. L. Núñez-Rico, B. Balakrishna, A. Vidal-Ferran, *RSC Adv.* **2014**, *4*, 58440–58447.
- [31] See the Supporting Information for further details.
- [32] Confirmed by mass-spectrometry analyses of the reaction mixture.
- [33] K. Nakano, G. Tatsumi, K. Nozaki, *J. Am. Chem. Soc.* **2007**, *129*, 15116–15117.
- [34] For the reactions of P/Al-based FLPs with propylene sulfide, see: a) W. Uhl, P. Wegener, M. Layh, A. Hepp, E.-U. Würthwein, *Organometallics* **2015**, *34*, 2455–2462; b) W. Uhl, J. Possart, A. Hepp, M. Layh, *Z. Anorg. Allg. Chem.* **2017**, *643*, 1016–1029.
- [35] G. M. Sheldrick, *Acta Cryst.* **2008**, *A64*, 112–122.
- [36] G. M. Sheldrick, *Acta Cryst.* **2015**, *A71*, 3–8.
- [37] G. M. Sheldrick, *Acta Cryst.* **2015**, *C71*, 3–8.
- [38] S. Parson, H. D. Flack, T. Wagner, *Acta Cryst.* **2013**, *B69*, 249–259.
- [39] A. L. Spek, *Acta Cryst.* **2009**, *D65*, 148–155.

Entry for the Table of Contents

FULL PAPER



Tetiana Krachko, Emmanuel Nicolas,
Andreas W. Ehlers, Martin Nieger, and
J. Chris Sootweg*

Page No. – Page No.

Ring-opening of Epoxides Mediated
by Frustrated Lewis Pairs

The stoichiometric reactions of methylene- (right) and *o*-phenylene-bridged (left) P/B-based frustrated Lewis pairs with mono-substituted epoxides result in epoxide ring-opening and the formation of six- and seven-membered heterocycles, respectively. In addition, insights into the reaction mechanism are provided based on DFT calculations as well as kinetic analyses.